Impact of late-Holocene aridification trend, climate variability and geodynamic control on the environment from a coastal area in SW Spain

10 authors, including:

Gonzalo Jiménez-Moreno
University of Granada
188 PUBLICATIONS **4,621** CITATIONS

SEE PROFILE

Antonio Rodríguez-Ramírez
Universidad de Huelva
103 PUBLICATIONS **1,258** CITATIONS

SEE PROFILE

José Noel Pérez-Asensio
University of Granada
52 PUBLICATIONS **734** CITATIONS

SEE PROFILE

José Carrión
University of Murcia
324 PUBLICATIONS **13,147** CITATIONS

SEE PROFILE

Impact of late-Holocene aridification trend, climate variability and geodynamic control on the environment from a coastal area in SW Spain

Gonzalo Jiménez-Moreno,[1] Antonio Rodríguez-Ramírez,[2]
José N Pérez-Asensio,[3] José S Carrión,[4] José Antonio López-Sáez,[5]
Juan JR Villarías-Robles,[6] Sebastián Celestino-Pérez,[7]
Enrique Cerrillo-Cuenca,[7] Ángel León[8] and Carmen Contreras[2]

Abstract
A detailed pollen analysis has been carried out on two sediment cores taken from a marsh area located in the Doñana National Park, southwestern Spain. The studied sedimentary sequences contain a similar late Holocene record of vegetation and climate and show a progressive aridification trend since at least 5000 cal. yr BP, through a decrease in forest cover in this area. Long-term vegetation changes shown here (semi-desert expansion and Mediterranean forest decline) paralleled declining summer insolation. Decreasing summer insolation most likely impacted negatively on tree growing season as well as on winter precipitation in the area. Superimposed on the long-term aridification trend were multi-centennial scale periods characterized by forest reductions or increases in arid and halophytic plants that can be interpreted as produced by enhanced droughts and/or by local geodynamic processes. These are centered at ca. 4000, 3000–2500, and 1000 cal. yr BP, coinciding in timing and duration with well-known dry events in the western Mediterranean and other areas but could have also been generated by local sedimentary or geodynamic processes such as a marine transgression in a subsidence context and extreme wave events (EWEs). The alternation of persistent North Atlantic Oscillation modes probably played an important role in controlling these relatively humid–arid cycles.

Introduction

Future climate reconstructions indicate that the western Mediterranean, including all of the Iberian Peninsula, will be warmer and drier (Hertig and Jacobeit, 2008; López-Moreno et al., 2011) with declining precipitation frequency (May, 2008). An important question to answer is how will vegetal environments respond to such climate changes in this area. Detailed paleoecological studies are necessary in order to understand the past relationship between climate, geodynamic control, vegetation, and human impact. In this respect, pollen analyses from marine and terrestrial sediment cores from the western Mediterranean area have been proven to be very informative about this matter (Anderson et al., 2011; Gil-Romera et al., 2010). These studies show a progressive aridification trend that started at ca. 5000 cal. yr BP and lasted until present (Jalut et al., 2009). This trend has been related to a decrease in summer insolation that occurred after the Holocene climatic optimum (Jiménez-Moreno and Anderson, 2012). In addition, this long-term trend is interrupted by millennial- and centennial-scale climatic oscillations that also affected the vegetation (Fletcher et al., 2013). Some of these variations have been suggested to be caused by alternation of persistent North Atlantic Oscillation (NAO) modes (Fletcher et al., 2013; Jiménez-Moreno et al., 2013).

The western Mediterranean area has a long history of human cultures and societies (Barker, 2005). However, the role that

[1]Departamento de Estratigrafía y Paleontología, Universidad de Granada, Spain
[2]Departamento de Geodinámica y Paleontología, Universidad de Huelva, Spain
[3]University of Geneva, Switzerland
[4]Departamento de Biología Vegetal, Universidad de Murcia, Spain
[5]Instituto de Historia, Centro de Ciencias Humanas y Sociales (CCHS), Consejo Superior de Investigaciones Científicas (CSIC), Spain
[6]Instituto de Lengua, Literatura y Antropología, Centro de Ciencias Humanas y Sociales (CCHS), Consejo Superior de Investigaciones Científicas (CSIC), Spain
[7]Instituto de Arqueología de Mérida, Consejo Superior de Investigaciones Científicas (CSIC), Spain
[8]Fundación del Hogar del Empleado (FUHEM), Spain

Corresponding author:
Gonzalo Jiménez-Moreno, Departamento de Estratigrafía y Paleontología, Universidad de Granada, Avda. Fuente Nueva S/N, Granada, 18002, Spain.
Email: gonzaloj@ugr.es

humans had and how much they contributed to the aridification process through their attempt to modify the landscape is still unknown (Bellin et al., 2013; Carrión et al., 2010). Several studies show that environmental changes were mostly induced by climate and humans had a relatively discrete and local role until the last millennia (Anderson et al., 2011; Bellin et al., 2013). In addition, other more local processes such as geodynamics could have altered the environment in the last millennia, complicating the interpretation of the environmental proxy records. This is especially important in estuaries with coastal barriers, where high-energy events and changes in sedimentary conditions are frequent (Hindson and Andrade, 1999; Kortekaas and Dawson, 2007; Ruiz Pessenda et al., 2012).

Southern Iberia is located in an important climatic boundary between the temperate and humid climate to the north and the subtropical, arid climate to the south. Moreover, Mediterranean forests have been proven to be very sensitive to Northern Hemisphere climate variability (Fletcher et al., 2013; Tzedakis, 2007). Nevertheless, relatively arid climate characterizes southern Spain (see below) and thus continuous Holocene pollen sequences are rare (see references below). In this respect, the Doñana National Park (Guadalquivir estuary, SW Spain) bears wetlands (coastal marshes and lagoons) that contain sediments deposited more or less continuously throughout the Holocene (Lario et al., 2002; Rodríguez-Ramírez et al., 2014; Salvany et al., 2011). Pollen records are thus available from the area since the 1960s (Laguna de Las Madres: Menéndez Amor and Florschütz, 1964; Stevenson, 1985; Stevenson and Harrison, 1992; Stevenson and Moore, 1988; Yll et al., 2003; El Acebrón: Stevenson and Harrison, 1992; Stevenson and Moore, 1988; Mari López: Yáñez et al., 2006; Yll et al., 2003; Las Marismillas: Yll et al., 2003; and El Asperillo: Caratini and Viguier, 1973; Stevenson, 1984). However, most of these studies are relatively low resolution and/or their age control is not very accurate.

Here, we present two pollen records from a marsh area in the Doñana National Park. This area was characterized by continuous sedimentation but also subjected to geodynamic processes such as subsidence, marine transgression, and marine inputs during EWEs (Rodríguez-Ramírez et al., 2014, in press). In this study, we concentrate on the last ca. 5000 cal. yr BP of vegetation, climate, and geodynamic history from this marshland in SW Spain and more regionally from the western Mediterranean, through a comparison of our pollen data with other records available for the area.

Physical environment

The study area is located in the Guadalquivir estuary, SW Iberia (Figure 1). The Doñana National Park is an area of marsh, shallow streams, sand dunes, scrub woodland, and maquis very famous among ornithologists as one of the largest heronries in the Mediterranean region and is the wintering site for more than 500,000 waterfowls each year (http://www.magrama.gob.es/es/red-parques-nacionales/nuestros-parques/donana/). The studied S7 and S11 cores (36°56′30″N, 6°24′48″W; 36°58′11″N, 6°47′98″W, respectively) are located in a marsh area at an elevation around 2 m.a.s.l. and only separated by ca. 3 km from each other (Figure 1).

The climate in this area is of Mediterranean type with hot and dry summers and mild winters. Most of the precipitation falls during the winter. Mean annual temperature is 16.7°C and precipitation is 537 mm (Doñana palace weather station; Yll et al., 2003). SW winds prevail in this area, with 22.5% of the days per year with wind in this direction (data of the National Meteorological Institute for the city of Huelva: 1960–1990; Rodríguez-Ramírez et al., 2003).

Vegetation in the study area belongs to the 'dry thermomediterranean' type (Rivas-Martínez, 1987). It is characterized by *Olea europaea* var. *sylvestris*, *Quercus coccifera*, *Q. rotundifolia*,

Q. suber, *Juniperus macrocarpa*, *J. phoenicea* var. *oophora*, and *Pinus pinea* as the most abundant tree species. *Pistacia lentiscus*, Cistaceae, *Phillyrea angustifolia, Rhamnus* spp., *Rosmarinus officinalis*, *Ruscus aculeatus*, *Thymus vulgaris*, *Asparagus* spp., *Daphne gnidium*, Ericaceae, and *Chamaerops humilis* are also abundant and characterize the Mediterranean scrub (Rivas-Martínez et al., 1980). Wetlands bear hydrophytic plants including Cyperaceae (*Cladium mariscus*, *Scirpus maritimus*, and *S. lacustris*), *Typha, Hydrocotyle, Phragmites*, and ferns (*Dryopteris* and *Thelypteris*). Inter-dune areas are covered by *Armeria arenaria*, *Carex*, and *Artemisia campestris*. In the salt marsh areas, the dominant vegetation is Amaranthaceae (mostly *Suaeda*) and *Juncus*. Reforestation with *Pinus pinea* and cultivated areas with *Fragaria ananassa* (strawberries) also occur in the surroundings (Rivas-Martínez et al., 1980).

The studied marsh

The Guadalquivir freshwater marshland is located in the Gulf of Cádiz and is one of the largest in Europe, with an area of 185,000 ha. This marshland is separated from the Atlantic Ocean by the Abalario dune systems and two coastal barriers or spits: 'Doñana and La Algaida' (Figure 1). There is a close connection between the development of the coastal barriers and the generation of the present-day marshland (Rodríguez-Ramírez et al., 1996). Four younger semi-mobile and mobile eolian dunes that accumulated mostly after the middle Holocene and can be up to 100 m high characterize the Abalario dune system. Two of the younger dunes are extended on the littoral spits and are related with littoral progradation phases (Rodríguez-Ramírez et al., 1996). The marshland is characterized by various muddy sedimentary bodies (levees, channels, and point-bars) that have resulted from intense fluvial action, extensive sandy, and shelly ridges (cheniers) resting on the clayey sediments and marine processes operating against the barriers (Rodríguez-Ramírez and Yáñez, 2008). The fluvial levees flank the river and its former courses above the adjacent interlevee marshes. These levees are part of a deltaic system that has been filling the old estuary. S7 and S11 cores are located in these interlevee areas where subsidence favored continuous sedimentation throughout the late Holocene. Marine inputs (EWEs) characterize the earliest part of the sedimentary record (Rodríguez-Ramírez et al., in press).

Materials and methods

Two sediment cores, S7 and S11, were taken in 2009 from the studied marsh area using a rotation-drilling machine. S11 was the longest core with 18 m. S7 was shorter, with a length of 12 m (Figure 2). Cores were transported back to the Universidad de Huelva, where they were stored and sampled for various proxies including radiocarbon dating and pollen analysis.

Core chronologies were developed using calibrated AMS radiocarbon dates (Table 1; Figures 2 and 3). Material for AMS dates consisted of mollusk shells and one organic bulk sediment sample from the S11 core. Samples for dating were initially dried and weighed before analysis. Radiocarbon ages were calibrated to 'calendar ages' using Calib 6.0 (IntCal09.14; Reimer et al., 2009). Correction of the reservoir effect followed AMM Soares' guidelines regarding calibration of marine shells from the Gulf of Cádiz (Soares and Martins, 2010; Table 1). We used linear interpolation to calculate the age–depth model for the two cores (Figure 3).

Samples for pollen analysis (1 cm³) were taken every 50 cm throughout the studied cores (Figures 4 and 5). Pollen extraction followed a modified Faegri and Iversen (1989) methodology using HF and HCl for mineral digestion and sieving and Zn_2Cl for density separation. Counting was performed at 400× – magnification to a minimum pollen sum of 300 terrestrial pollen grains. The raw
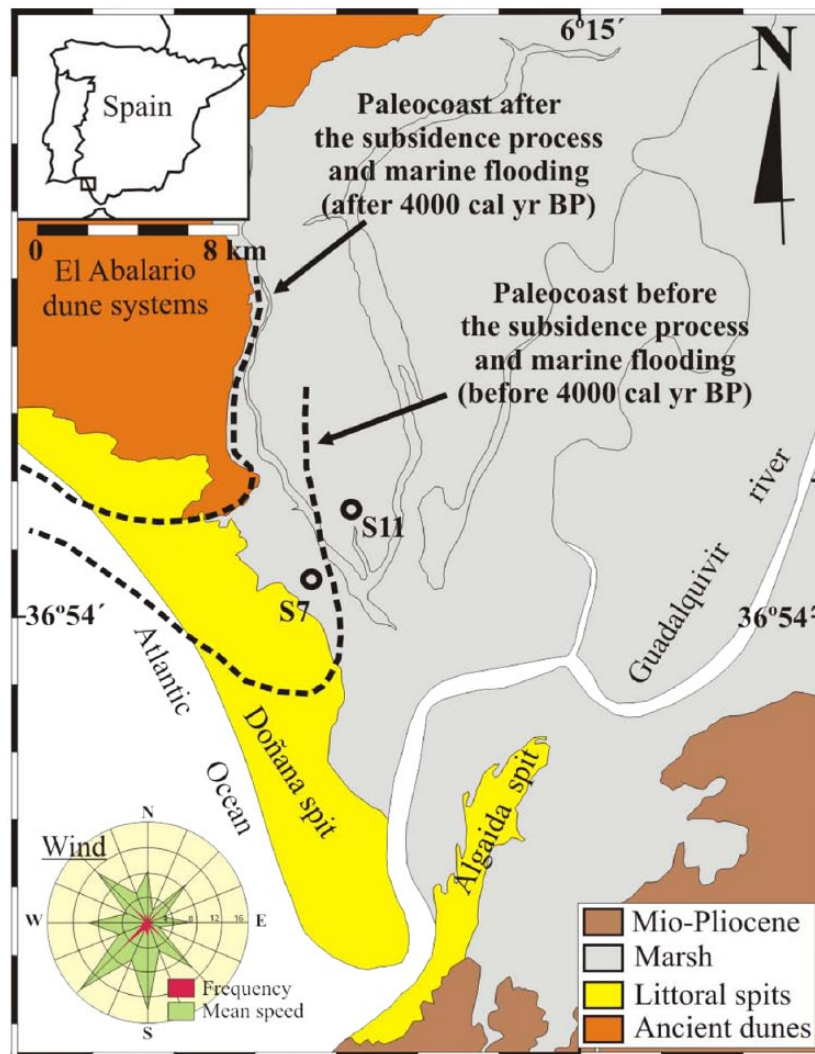
Figure 1. Location of core sites S7 and S11 in the *marismas* (marshland) of the Doñana National Park, SW Spain. The interpreted paleocoast before and after 4000 cal. yr BP is indicated (Rodríguez-Ramírez et al., 2014).

**Table 1.** Age data for S7 and S11 cores, SW Spain.

Lab number[a]	Core	Depth (cm)	Material dated	δ^{13}C (‰)	Age (^{14}C yr BP ± 1σ)	Calibrated age (cal. BP) 2σ ranges	Median
	S7	0			Present	AD 2009	−59
Beta-285000	S7	250	Shell	0.1	3370 ± 40	2824–3360	3092
Beta-285001	S7	550	Shell	0.4	3780 ± 40	3346–3871	3608
Beta-285002	S7	800	Shell	1.3	4040 ± 40	3633–4230	3931
	S11	0			Present	AD 2009	−59
D-AMS 001534	S11	350	Shell	12.10	3383 ± 28	2845–3363	3104
Beta-285006	S11	400	Shell	−2.5	3190 ± 40	2672–3194	2933
D-AMS 002422	S11	700	Shell	−4.6	3596 ± 60	3073–3669	3371
D-AMS 001536	S11	750	Shell	7.60	3918 ± 25	3502–4058	3780
D-AMS 001537	S11	850	Shell	5.50	3781 ± 33	3352–3862	3607
D-AMS 001538	S11	1150	Shell	2.90	4260 ± 30	3931–4510	4220
Beta-285007	S11	1250	Shell	−0.3	4860 ± 40	5256–5460	5046
Beta-285008	S11	1350	Bulk organic sediment	−25.2	19360 ± 80		

All dates were calibrated using Calib 6.0 (Reimer et al., 2009). For marine shell samples, we used a reservoir $\Delta R = 100 \pm 100$ and $\Delta R = -135 \pm 20$ for Beta-285007 (Soares and Martins, 2010). In red are the dates that were considered too old and were not used in the age model.
[a]Sample number assigned at radiocarbon laboratory; D-AMS#: Accium Biosciences, Seattle, WA; Beta#: Beta Analytic.

counts were transformed to pollen percentages based on the pollen sum. A summary of important pollen types (higher abundances than 1%) for cores S7 and S11 is plotted in Figures 4 and 5, respectively. Percentages of dinoflagellate cysts (dinocysts) were calculated with respect to the total pollen+dinocysts sum and are shown in Figures 4 and 5. The same was applied for *Isoetes*, and
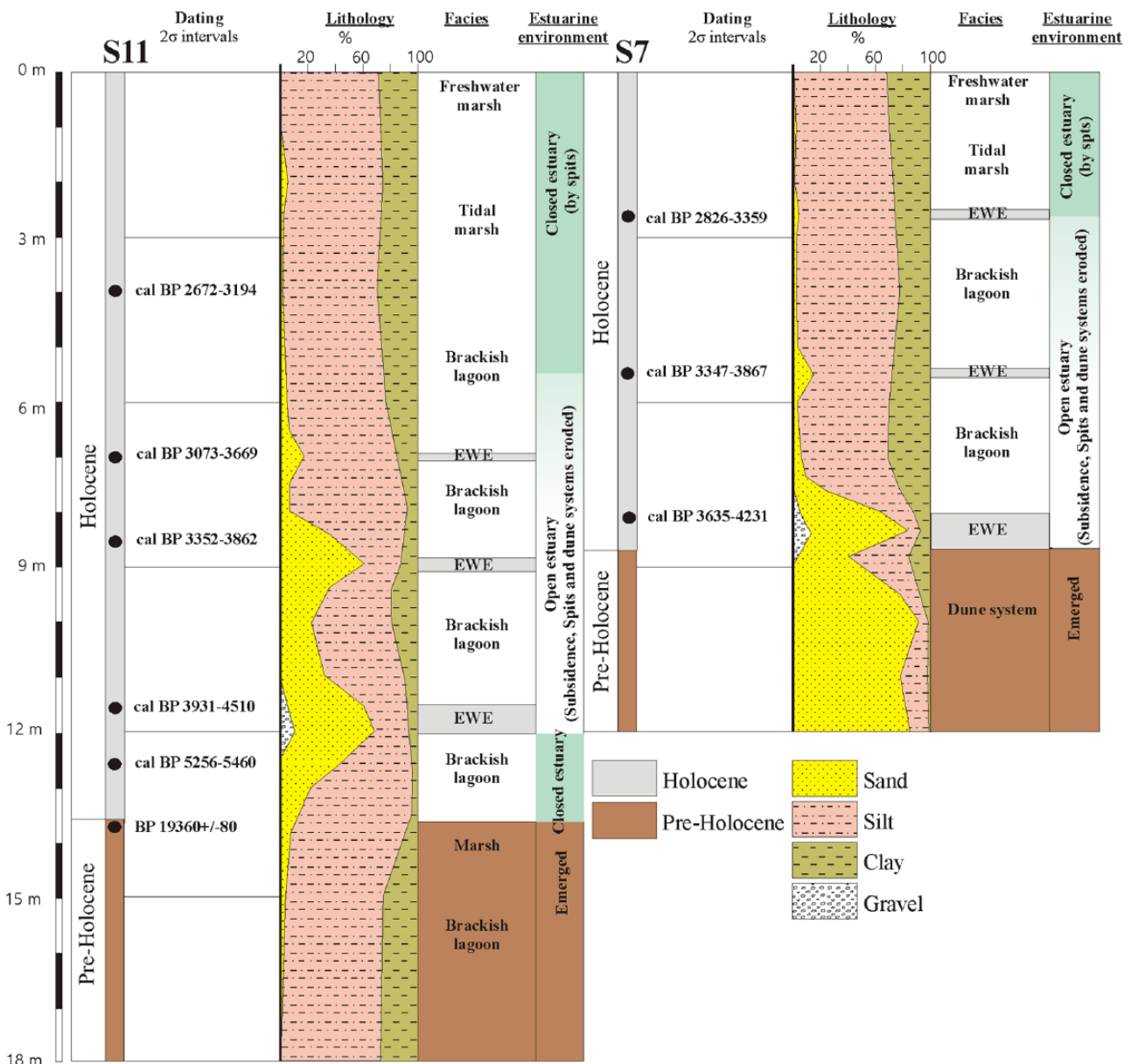
Figure 2. Lithologic logs and location of radiocarbon dates from cores S7 and S11.

its percentage was calculated with respect to the pollen+*Isoetes* sum. Arboreal pollen (AP)/arid (*Artemisia*+Amaranthaceae) ratios were calculated for both the S11 and S7 pollen records (shown in Figure 6). We use this relationship to document forest versus steppe fluctuations during the Holocene (i.e. Jiménez-Moreno et al., 2011). The ratio was calculated following the equation: AP/arid ratio=(AP−arid)/(AP+arid). Average AP/arid ratio values between the resampled AP/arid ratios by linear interpolation from S11 and S7 cores were calculated using Analyseries 2.0 (Paillard et al., 1996).

Results

Chronology and sedimentary rates

Eleven calibrated radiocarbon ages were used to determine the sediment chronologies from S7 and S11 (Table 1; Figure 3). Age models from both records seem to show very similar sedimentary rates (Figure 3). The age–depth model for the S7 and S11 cores suggests that sedimentation was more or less continuous in the marsh area for at least the last ca. 5000–4000 cal. yr BP (Figures 2 and 3). Radiometric dates from the S11 core show two seemingly old ages of 3104 and 3780 cal. yr BP at 350 and 750 cm,

respectively. We attribute this to mobilization and re-sedimentation of old organic material into the marsh area probably due to the EWEs. Those radiocarbon ages were not used in the age-model construction. Sediment accumulation rates (SAR) were calculated between the radiocarbon dates. Relatively low SARs characterize the earliest part of the S11 record, with values around 1.21 mm/yr. SARs increased substantially later on, between 4000 and 3000 cal. yr BP, with values between ca. 4.89 and 7.69 mm/yr. Both records show relatively low SAR in the last ca. 3000 cal. yr BP, between 0.79 and 1.33 mm/yr (Figure 3).

Lithology

The lower part of core S11, from −18 to −13.5 m, is a typical marsh sequence of mostly clayey silts (70–75% silts, 20–25% clay, and 2–5% sand) of a grayish ocher (10YR8/2) color, with burrowing, roots, carbonate nodules, oxidation, and intense lamination. The lower portion of core S7, from −12 to −8.5 m, consists of a sequence of fine to medium sands (75–90% sand, 5–20% silts, and 1–4% clay), well sorted (≈65–70% around 0.125–0.5 mm), white-orangish (10YR7/8) in color, and containing abundant red stains, roots, and bioturbation.

The dominant lithology in the two cores is gray-greenish (10YR6/1) clayey silts: 50–60% silts, 15–35% clay, and 10–1% sand, with more ocher tones (10YR6/4) in the upper 2 m. The
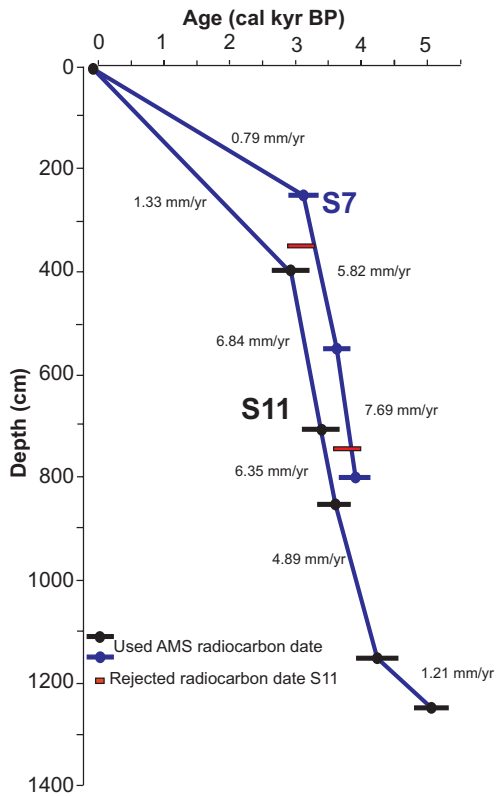

Figure 3. Age–depth diagram and sedimentary rates for the S7 and S11 sediment records. In red are dates that were not used in the age model for the S11 core.

lower part of S11 presents the largest amounts of sand content (20–30% sand) from −13.5 to −7.5 m, turning progressively into clayey silts toward the top (<1% sand). The mollusk and gastropod macrofauna appear to be dominated by shallow water estuarine fauna from sheltered environments (*Tellina tenuis*, *Cerastoderma edule*, *Saccostrea virletii*, *Nassarius* sp.). Different decimetric layers with higher sand content and abundant marine mollusks and gastropods appeared in the different cores in relation to marine inputs. The macrofauna is composed of a mixture of disarticulated valves, shell fragments, and whole bivalves, with a high diversity of marine (*Glycymeris* sp., *Chlamys* sp., *Cardidae* sp., *Anomia ephippium*, and *Bittium reticulatum*) and estuarine species (*Cerastoderma edule* and *Saccostrea virletii*).

Pollen, dinocysts, and algae

Sixty different pollen, two algal species (*Botryococcus* and *Pediastrum*), microspores of *Isoetes*, and different species of dinocysts have been identified in the S7 and S11 cores. Some of the identified pollen taxa and algae occur in percentages lower than 1% and have not been plotted in Figures 4 and 5. Both pollen records show low percentages of arboreal forest taxa (%AP), with mean values around 15–20%, mostly made up of *Pinus*, *Quercus* (both evergreen and deciduous), *Olea*, and *Juniperus*. Herbs and grasses such as Amaranthaceae, Poaceae, and Asteraceae (including *Artemisia*, Asteraceae Cichorioideae, and other Asteraceae) dominate the pollen spectra. Ericaceae shrubs are present with varying abundances around 5%. Hydro-hydrophytic taxa also occur and are mostly represented by Cyperaceae, *Myriophyllum*, and *Isoetes*. Dinocysts are dominated by *Lingulodinium machaerophorum* but *Spiniferites* sp. and *Hystrichokolpoma rigaudiae* are also present.

S11 and S7 pollen records show quite similar results with respect to long-term pollen variations. The earliest part of both records is characterized by maxima in %AP as well as in *Isoetes* and dinocysts. The S11 core is older and shows %AP around
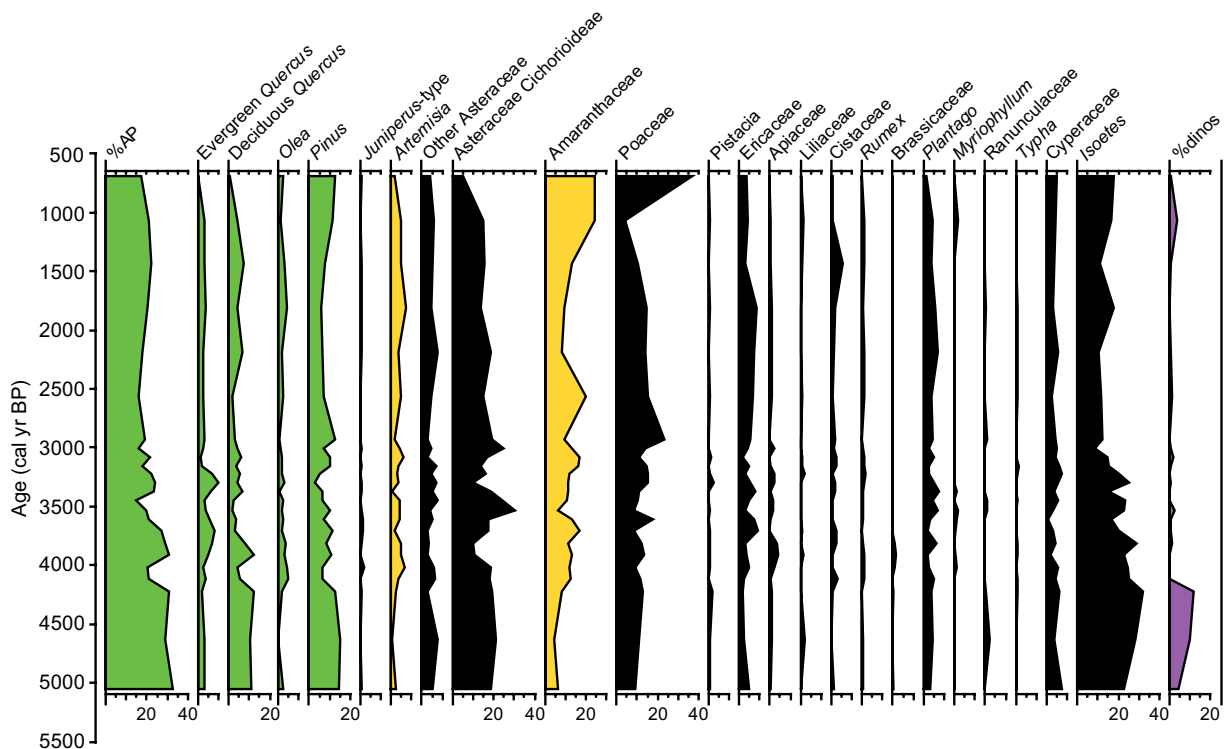
Figure 4. Pollen diagram of the S11 record showing percentages of selected taxa (higher than 1%). *Isoetes* and dinocyst percentages were calculated with respect to the total pollen sum. AP was calculated adding the percentages of *Pinus*, *Quercus*, *Juniperus*, *Olea*, *Fraxinus*, *Ulmus*, *Abies*, *Alnus*, *Betula*, and *Juglans*.
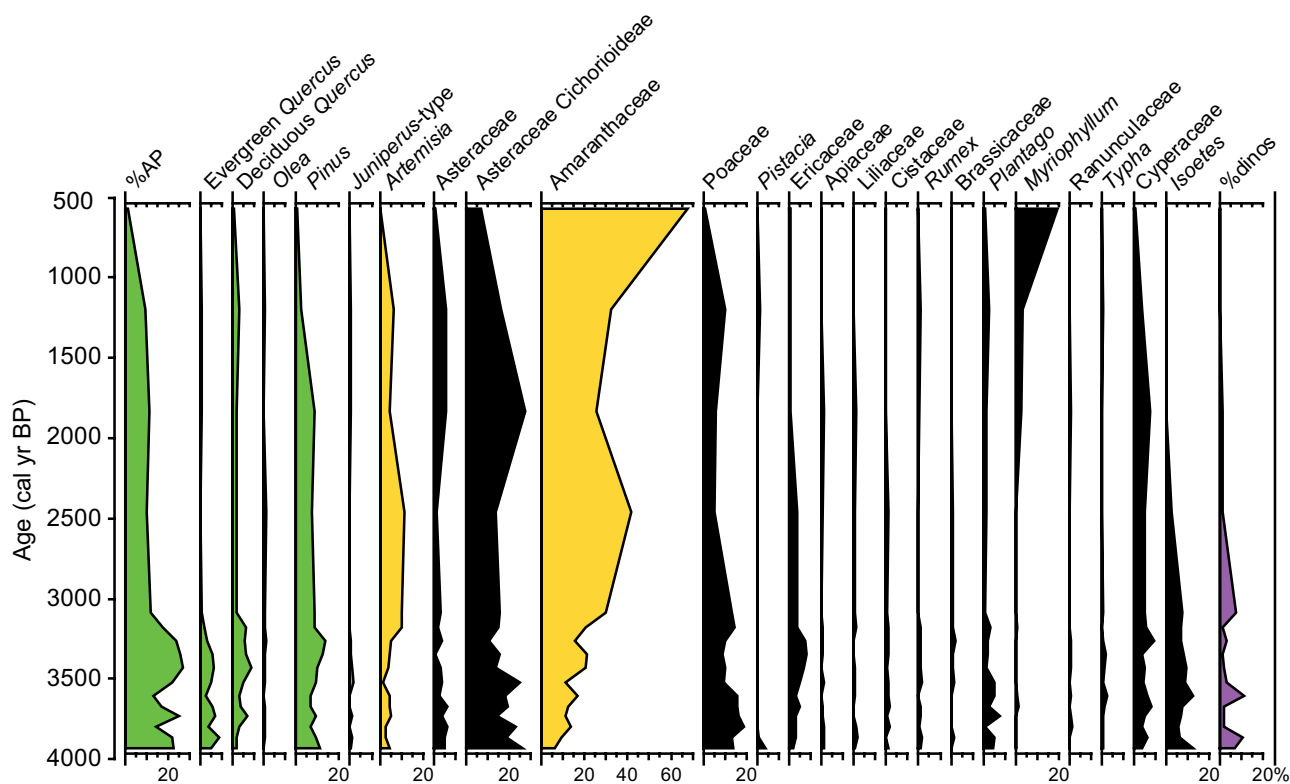
Figure 5. Pollen diagram of the S7 record showing percentages of selected taxa (higher than 1%). *Isoetes* and dinocyst percentages were calculated with respect to the total pollen sum. AP was calculated adding the percentages of *Pinus, Quercus, Juniperus, Olea, Fraxinus, Ulmus, Abies, Alnus, Betula,* and *Juglans*.

30% between 5000 and 4300 cal. yr BP. A decreasing trend is observed since then until the last centuries in both records: from ca. 30% to ca. 20% in the S11 and from ca. 20% to ca. 5% in the S7. This trend is mostly triggered by decreasing *Quercus* and *Pinus* (in the S7 record) and an increase in Amaranthaceae (from 5% to 25% in the S11 and from 10% to 65% in the S7) and in *Artemisia. Isoetes* and dinocysts also decreased throughout the late Holocene in both records.

Shorter-term scale changes are also observed in both records. These variations are clearly recorded in the AP/arid ratio (Figure 6). Minima in AP/arid ratios in an average plot of the %AP of the two records are reached at ca. 4000, 3000–2500, and 1000 cal. yr BP.

Discussion

### Middle and late Holocene aridity trend and geodynamics

Maxima in warm and humid conditions characterized the early–middle Holocene (following the subdivision by Walker et al., 2012) from ca. 10,500–7000 cal. yr BP in the western Mediterranean area (Anderson et al., 2011; Jalut et al., 2009; Jiménez-Moreno and Anderson, 2012). Pollen records from southwestern Iberia also indicate optimum climate conditions, with a maximum development of *Quercus* forest and thermomediterranean evergreen taxa between ca. 10,000 and 6500 cal. yr BP (Fletcher et al., 2007; Reed et al., 2001; Santos et al., 2003). Highest sea level is also observed in coastal sedimentary sequences in this area (i.e. the Flandrian maximum; Zazo et al., 1994).

The Holocene climatic optimum can be explained by orbital-scale summer insolation maxima (Laskar et al., 2004). This contributed to climate warming, generating an increase in the land–sea contrast that would trigger enhanced wind system and higher precipitations during fall–winter season (Meijer and Tuenter, 2007; Tuenter et al., 2003). Also, a reorganization of the

general atmospheric circulation with a southward shift of the westerlies has been interpreted, inducing wetter conditions in this area (Magny et al., 2012).

Pollen data from S11 and S7 records show a decreasing trend in arboreal taxa (%AP) as early as the beginning of the records, ca. 5000 cal. yr BP (S11), and until the last centuries. Arid taxa such as Amaranthaceae and *Artemisia* increased considerably during this period (Figures 4–6). A progressive decrease in *Isoetes*, a shallow water aquatic plant, is also observed in both S11 and S7 records (Figures 4 and 5). All of this can probably be interpreted as an increase in aridity in the area, which would induce a forest reduction around the marsh and would trigger lower freshwater levels (Carrión et al., 2010) or more frequent instability or eutrophication in the marsh at that time. Aridification does seem to play the main role in transforming the vegetation in this region during the middle and late Holocene, as observed at many other pollen records from southern Spain and the Alboran Sea (Anderson et al., 2011; Carrión, 2002; Carrión et al., 2007, 2010; Combourieu-Nebout et al., 2009; Fletcher et al., 2007, 2013; Jiménez-Moreno and Anderson, 2012; Pérez-Obiol et al., 2011; see some of these records in Figure 6). All these pollen records show a more or less steep progressive reduction in forest species and the increase in herbaceous xerophytes (*Artemisia*, Amaranthaceae, and other herbs) at that time agreeing with our study.

Other climate proxy records from the area support the idea of a general trend to climatic aridification over the second half of the Holocene. For example, the lake-level investigations from Laguna de Medina and Laguna de Río Seco, which show more ephemeral and shallower lake levels since then (Jiménez-Espejo et al., 2014; Reed et al., 2001). A landscape evolution study in the Huelva coast shows that the onset of the accumulation of large mobile and semi-mobile dune systems, related to aridity in the area, began at ca. 5000 cal. yr BP (Zazo et al., 2005). A recent study from an alpine lake in the Sierra Nevada, in southern Spain, records a
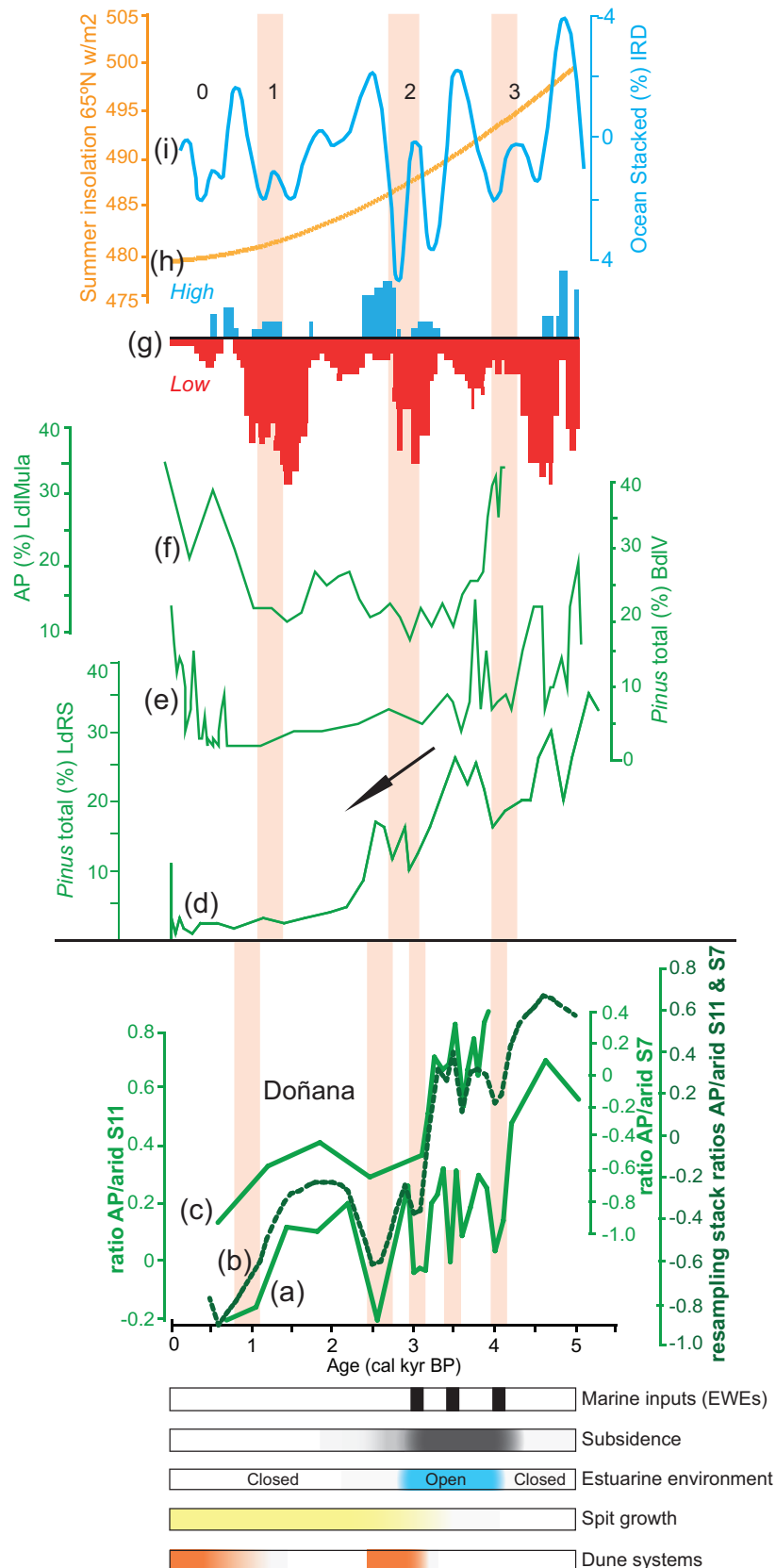
Figure 6. Comparison of pollen records from the western Mediterranean area with other paleoclimate proxies, including distant sites, for the last 5000 cal. yr BP. (a) AP/arid ratio from S11 core, Guadalquivir estuary, southern Spain. AP/arid ratio = (AP − arid)/(AP + arid). (b) Average plot between the resampled AP/arid ratios by linear interpolation from S11 and S7 cores (dashed line). (c) AP/arid ratio from S7 core, Guadalquivir estuary, southern Spain. (d) *Pinus* total from Laguna de Río Seco core (LdRS), Sierra Nevada, southern Spain (Anderson et al., 2011). (e) *Pinus* total from Borreguiles de la Virgen core (BdlV), Sierra Nevada, southern Spain (Jiménez-Moreno and Anderson, 2012). (f) AP from Laguna de la Mula (LdlMula), Sierra Nevada, southern Spain (Jiménez-Moreno et al., 2013). (g) Lake-level reconstruction for central Europe (Magny, 2004). Low and high lake levels are represented in red and blue, respectively. (h) Summer insolation at 65°N from Laskar et al. (2004). (i) Ocean stacked ice-rafting debris (IRD) from the North Atlantic (Bond et al., 2001). Numbers 0, 1, 2, and 3 indicate cold events. Arid events are highlighted with light red shading.

progressive increase in Saharan eolian dust deposition starting at ca. 7000–6000 cal. yr BP (Jiménez-Espejo et al., 2014). A marine record off northwestern Africa also shows a significant increase in eolian dust at around 5500 cal. yr BP, which was interpreted as the abrupt end of the African Humid Period (DeMenocal et al., 2000). Bellin et al. (2013) also reported enhanced geomorphic instability (i.e. high erosion and soil degradation) since 5600 cal. yr BP in SE Spain. Climate cooling after the early Holocene thermal maximum is also observed in sea-surface temperatures deduced from sediment marine cores from the area (Cacho et al., 2002).

The observed aridification trend during the middle and late Holocene seems to be related to the decreasing trend in summer insolation (Figure 6). Reduced summer insolation could have produced lower sea-surface temperatures (Marchal et al., 2002), generating a decrease in the land–sea contrast that would be reflected in a reduction of the wind system and lower precipitations during the fall–winter season. Also, a reorganization of the general atmospheric circulation with a northward shift of the westerlies – a long-term enhanced NAO+ trend – has been interpreted, inducing drier conditions in this area (Magny et al., 2012). Declining summer insolation at these latitudes would have negatively affected the growing season due to cooling, producing further forest decline (Fletcher et al., 2007).

Geodynamic processes also occurred in this coastal area, which triggered changes in the sedimentary and fossil record (Figures 2 and 6). Before ca. 4000 cal. yr BP, the estuary was mostly closed, and the landscape was characterized by a stabilized dune system around S7, while a brackish lagoon occurred around S11. The estuary opened to the ocean and fully became a brackish lagoon at ca. 4000 cal. yr BP due to enhanced subsidence. Subsidence was important between 4000 and 2000 cal. yr BP, and a significant area west of S7 and S11, the southernmost sector of the Abalario dunes, was flooded (Rodríguez-Ramírez et al., 2014; Figure 1). Marine inputs (i.e. during EWEs) bringing sand to the overall lutite sedimentation and enhanced sedimentary rates (between 4.9 and 7.7 mm/yr) occurred then. The gradual confinement of the Guadalquivir estuary since 3000–2800 cal. yr BP, produced by progradation of the littoral systems and infilling of the marshland, could have generated a progressively less influence of marine waters in the studied marsh (Rodríguez-Ramírez and Yáñez, 2008; Rodríguez-Ramírez et al., in press), inducing a decrease in the dinoflagellate cyst, transported marine benthic and planktonic foraminifera, and marine macrofauna, recorded in both S11 and S7 cores (Figures 4 and 5). Furthermore, benthic foraminifera from sheltered environments (e.g. *Haynesina germanica* assemblage; Murray, 2006; Pérez-Asensio and Aguirre, 2010; Ruiz et al., 2005) are more abundant in younger sediments in both cores (Rodríguez-Ramírez et al., in press). Since then, sedimentation in the estuary was more stable, with lower sedimentary rates (between 0.7 and 1.3 mm/yr) and characterized by more or less homogeneous lutites. Vegetation in the area could have been affected by these changes in the estuarine environment. These processes would have only affected immediate vegetation around the marsh or lagoon area, being this mostly characterized by herbs, halophytes (i.e. Amaranthaceae), and aquatic plants. However, the progressive linear trend observed in the pollen record since 5000 cal. yr BP does not seem to match with geodynamic changes, such as the closing–opening–closing of the estuary, which would produce a very clear cyclical-like pollen signal. It looks like our pollen records bear a strong component of regional pollen input coming in the area by wind or fluvial transport.

Millennial-scale variability

The S11 and S7 pollen records show that superimposed on the long-term aridification trend were multi-centennial scale periods characterized by decreases in the AP/arid ratios at ca. 4000, 3000–2500, and 1000 cal. yr BP (Figure 6). These decreases could be interpreted by either regional forest reductions caused by enhanced droughts and/or increases in herbs–halophytes that could be due to more local geodynamic processes. Comparing the S11 and S7 records with other pollen records from southern Spain showing millennial-scale variability (Laguna de Río Seco, Borreguiles de la Virgen, and Laguna de la Mula terrestrial records from the Sierra Nevada (Anderson et al., 2011; Jiménez-Moreno and Anderson, 2012; Jiménez-Moreno et al., 2013)) shows that some of the 'arid' steps identified in our records coincide in time and duration – within the error of the radiocarbon dating – with three regional arid events, centered at ca. 4200, 3000, and 1200 cal. yr BP, well known in the western Mediterranean and other areas (Figure 6). However, geodynamics are important in the area with enhanced subsidence at this time, and processes such as EWEs could have also controlled environment and vegetation change in the immediate area (Figure 6).

The ca. 4000 cal. yr BP step is shown in the S11 core by a reduction in AP/arid ratios and specifically in *Pinus* and deciduous *Quercus*, *Isoetes*, and dinocysts. This apparent forest reduction could have been due to regional climatic and/or more local environmental changes (or both). Climatically, a ca. 4200 cal. yr BP arid event is also observed in another regional paleoclimate proxy records, such in the lake records from Zoñar Lake and Siles Lake (Carrión, 2002; Martín-Puertas et al., 2008). Strong dryness is also observed more globally, for example, in Central Europe (Magny, 2004), Italy (Drysdale et al., 2006), the Red Sea (Arz et al., 2006), or North America (Booth et al., 2005), and some researchers relate this arid period with the collapse of the old Akkadian culture in Mesopotamia (Weiss et al., 1993), as well as the collapse of Neolithic Chinese cultures (An et al., 2005; Liu and Feng, 2012). This arid event coincides roughly with Bond's cold event 3 (Bond et al., 2001; Figure 6), event 3 of Wanner et al. (2011), and one of the six periods of significant rapid climate change of Mayewski et al. (2004). This ca. 4200 cal. yr BP climatic event marks the beginning of the Neoglacial (Wanner et al., 2011). Therefore, Walker et al. (2012) proposed it as a suitable marker to subdivide the Holocene period into 'middle' and 'late' chronozones. However, a marine input is also recorded at this time in the S11 and S7 by a sandy layer and has been interpreted as an EWE in a subsidence and marine transgressive context (see section above; Rodríguez-Ramírez et al., in press). This could have brought more salt in the marsh area and change the local vegetation toward more halophytic conditions (i.e. more Amaranthaceae), also triggering the decrease in AP/arid taxa.

The ca. 3000–2500 cal. yr BP step is also noticeable in the S11 record by two minima in AP/arid ratios, *Isoetes* and dinocysts around that age. This step is also obvious in the S7 core, but this record also shows reducing values in the AP/arid ratios together with a minimum in the dinocyst occurrence around 3000 cal. yr BP. This pollen oscillation could be interpreted climatically as enhanced aridification in the area. This would be supported by the ca. 3000 cal. yr BP arid event that has been locally recognized by a desiccation in the Laguna de Medina (Reed et al., 2001) and by accumulation of an eolian unit (U5) at ca. 2700 cal. yr BP in the nearby coastal area of El Abalario and Doñana (Zazo et al., 2005). It has also been regionally described by lower lake levels in Zoñar Lake and Siles Lake (Carrión, 2002; Martín-Puertas et al., 2008), also in a study by Bellin et al. (2013) who show enhanced geomorphic instability in the area (aridification event A2). Globally, this step coincides in time with Bond's cold event 2 from the North Atlantic (Bond et al., 2001), mayor global climatic reorganizations (Mayewski et al., 2004), and low lake levels in central Europe (Magny, 2004; Figure 6). Another EWE occurred in this estuarine area at this time (ca. 3000

cal. yr BP; Figure 6). This again could have caused the increase in herbs–halophytes triggering the decrease in AP/arid ratios (Figure 6) observed in the record.

Minima in AP/arid ratios pointing to another arid step also occurred at ca. 1000 cal. yr BP in the S11 record, agreeing with other pollen records regionally (Jiménez-Moreno et al., 2013). It looks like the last eolian accumulation phase in the nearby El Abalario and Doñana dunes occurred around this arid time (Figure 6). The ca. 1000 cal. yr BP arid step falls around the Dark Ages from ca. 1450 to ca. 1050 cal. yr BP and the Medieval Climate Anomaly (MCA; from ca. 1050 to ca. 700 cal. yr BP; Moreno et al., 2012) and occurred after the Roman Humid Period, also well documented in the area (Jiménez-Moreno et al., 2013; Martín-Puertas et al., 2010). Aridity around that time is observed in other pollen records from the region: in the Alboran Sea (MD95-2043 and ODP 976 cores; Combourieu-Nebout et al., 2009; Fletcher et al., 2013) and in the Guadiana Valley, Portugal (Fletcher et al., 2007). The Laguna de Medina record, Cádiz, documents desiccation events at that time (Reed et al., 2001), and the Mg/Al and Rb/Al ratios from the Alboran Sea and Lake Zoñar show a significant decline in precipitation (Martín-Puertas et al., 2010). Lake levels are also low at this time in southwestern and central Europe (Magny 2004; Martín-Puertas et al., 2010). This arid step coincides with cold sea-surface temperatures (event AC1) from the Alboran Sea (Cacho et al., 2002), Bond cold event 1 in the North Atlantic (Bond et al., 2001), and a period of significant rapid climate change of Mayewski et al. (2004).

This study shows millennial-scale variability in the late Holocene vegetation from the Guadalquivir estuary area that could have been caused by climate change. The comparison of these pollen records with another proxy records from the western Mediterranean area shows millennial-scale climatic periods that seem to be recognized regionally and globally, for example, in the North Atlantic. This would support the hypothesis of a highly efficient climatic coupling between the North Atlantic and the western Mediterranean region during the late Holocene. The NAO is one of the major climate modes that naturally affect weather and climate patterns across Europe, controlling winter precipitation in the area (Hurrell, 1995). Positive NAO years are associated with Iberian dryness and cold temperatures in Greenland (Frigola et al., 2007; Hurrell, 1995). Therefore, the arid steps recognized in the paleoclimate records from the western Mediterranean area could be related with periods of persistent positive NAO index, triggering a northward migration of the westerlies and less winter precipitation in the region (Frigola et al., 2007; Muñoz-Díaz and Rodrigo, 2003).

In the Guadalquivir estuary, such global climatic changes may have compounded the effects of local geodynamic processes such as a marine transgression and EWEs on the pollen record, especially for the ca. 4000 and 3000 cal. yr BP events (Figure 6). We think that in both cases, regional climate (i.e. aridity) and/or local coastal processes (i.e. EWEs) would generate a similar effect on the pollen record, an increase in herbs and, in particular, in Amaranthaceae, and then could have been combined. In addition, historical records make reference to a large tsunami that hit the coasts of SW Iberia in AD 881 (Guidoboni et al., 1994) but does not seem to be recorded in our sedimentary records. Very active storms over the North Atlantic during persistent NAO+ periods could have generated abundant cyclones in the area (Nissen et al., 2010), perhaps explaining the occurrence of EWEs at those times. However, this does not exclude the possibility of tsunamigenic origin of some of these EWEs, as suggested by Rodríguez-Ramírez et al. (in press). This study then shows that estuarine environments in tectonically active areas are, therefore, particularly complex when trying to learn about climatic patterns and their effects on the vegetation.

Conclusion

Pollen and other paleoclimate records from SW Spain and the western Mediterranean show a clear aridity trend during the middle and late Holocene. This is shown in the pollen records through a loss of forest cover and the increase in xerophytic herbs. The aridity trend seems to be caused by a decrease in insolation that occurred at that time, triggering lower sea-surface temperatures and a decrease in the land–sea contrast that would generate a reduction of the wind system and lower precipitations during the fall–winter season. Also, a reorganization of the general atmospheric circulation with a northward shift of the westerlies – a long-term enhanced NAO+ trend – has been interpreted, inducing drier conditions in this area.

The studied records also show millennial-scale variability, identifying three main periods characterized by forest reduction and/or increase in arid plant species and halophytes. These climatic steps were centered at ca. 4000, 3000–2500, and 1000 cal. yr BP, coinciding in timing and duration with well-known arid events in the western Mediterranean and other areas such as the North Atlantic. This suggests that vegetation changes in this area could have been triggered by millennial-scale climate variability, supporting a highly efficient climatic coupling between the North Atlantic and the western Mediterranean and alternation of persistent NAO+ and NAO− modes as the main mechanism forcing millennial-scale precipitation changes. Another explanation for the Guadalquivir estuary pollen variations could be more related with local geodynamic processes such as marine transgression over the Abalario dune systems and two EWEs, which occurred during two of these steps (ca. 4000 and 3000 cal. yr BP). We think that both processes, regional climate and local geodynamics, would have produced a similar pattern on the pollen record and may have combined, which makes this tectonically active estuarine environment tricky when trying to understand vegetation variations due to climate change.

References

An CB, Tang L, Barton L et al. (2005) Climate change and cultural response around 4000 cal yr B.P. in the western part of Chinese Loess Plateau. *Quaternary Research* 63: 347–352.

Anderson RS, Jiménez-Moreno G, Carrión JS et al. (2011) Holocene vegetation history from Laguna de Río Seco, Sierra Nevada, Southern Spain. *Quaternary Science Reviews* 30: 1615–1629.

Arz HW, Lamy F and Pätzold J (2006) A pronounced dry event recorded around 4.2 ka in brine sediments from the northern Red Sea. *Quaternary Research* 66: 432–441.

Barker G (2005) Agriculture, pastoralism, and Mediterranean landscapes in prehistory. In: Blake E and AB Knapp (eds) *The Archaeology of Mediterranean Prehistory*. Oxford: Blackwell, pp. 46–76.

Bellin N, Vanacker V and de Baets S (2013) Anthropogenic and climatic impact on Holocene sediment dynamics in SE Spain: A review. *Quaternary International* 308–309: 112–129.

Bond G, Kromer B, Beer J et al. (2001) Persistent solar influence on North Atlantic climate during the Holocene. *Science* 294: 2130–2136.

Booth RK, Jackson ST, Forman SL et al. (2005) A severe centennial-scale drought in midcontinental North America 4200 years ago and apparent global linkages. *The Holocene* 15: 321–328.

Cacho I, Grimalt JO and Canals M (2002) Response of the Western Mediterranean Sea to rapid climatic variability during the last 50,000 years: A molecular biomarker approach. *Journal of Marine Systems* 33–34: 253–272.

Caratini C and Viguier C (1973) Étude palynologique et sédimentologique des sables holocènes de la falaise littorale d'El Asperillo (Province de Huelva). *Estudios Geológicos* 29: 325–328.

Carrión JS (2002) Patterns and processes of Late Quaternary environmental change in a montane region of Southwestern Europe. *Quaternary Science Reviews* 21: 2047–2066.

Carrión JS, Fernández S, González-Sampériz P et al. (2010) Expected trends and surprises in the Lateglacial and Holocene vegetation history of the Iberian Peninsula and Balearic Islands. *Review of Palaeobotany and Palynology* 162: 458–476.

Carrión JS, Fuentes N, González-Sampériz P et al. (2007) Holocene environmental change in a montane region of Southern Europe with a long history of human settlement. *Quaternary Science Reviews* 26: 1455–1475.

Combourieu-Nebout N, Peyron O, Dormoy I et al. (2009) Rapid climatic variability in the west Mediterranean during the last 25000 years from high resolution pollen data. *Climate of the Past* 5: 503–521.

DeMenocal P, Ortiz J, Guilderson T et al. (2000) Abrupt onset and termination of the African Humid Period: Rapid climate responses to gradual insolation forcing. *Quaternary Science Reviews* 19: 347–361.

Drysdale R, Zanchetta G, Hellstrom J et al. (2006) Late Holocene drought responsible for the collapse of Old World civilizations is recorded in an Italian cave flowstone. *Geology* 34: 101–104.

Faegri K and Iversen J (1989) *Textbook of Pollen Analysis*. New York: Wiley.

Fletcher W, Boski T and Moura D (2007) Palynological evidence for environmental and climatic change in the lower Guadiana valley (Portugal) during the last 13,000 years. *The Holocene* 17: 479–492.

Fletcher WJ, Debret M and Sánchez Goñi MF (2013) Mid-Holocene emergence of a low-frequency millennial oscillation in western Mediterranean climate: Implications for past dynamics of the North Atlantic atmospheric westerlies. *The Holocene* 23: 153–166.

Frigola J, Moreno A, Cacho I et al. (2007) Holocene climate variability in the western Mediterranean region from a deepwater sediment record. *Paleoceanography* 22: PA2209.

Gil-Romera G, Carrión JS, Pausas JG et al. (2010) Holocene fire activity and vegetation response in South-Eastern Iberia. *Quaternary Science Reviews* 29: 1082–1092.

Guidoboni E, Comastri A and Traina G (1994) *Catalogue of Ancient Earthquakes in the Mediterranean Area up to the 10th Century*. Rome: Istituto Nazionale di Geofisica.

Hertig E and Jacobeit J (2008) Downscaling future climate change: Temperature scenarios for the Mediterranean area. *Global and Planetary Change* 63: 127–131.

Hindson RA and Andrade C (1999) Sedimentation and hydrodynamic processes associated with the tsunami generated by the 1755 Lisbon earthquake. *Quaternary International* 56: 27–38.

Hurrell JW (1995) Decadal trends in the North Atlantic Oscillation: Regional temperatures and precipitation. *Science* 269: 676–679.

Jalut G, Dedoubat JJ, Fontugne M et al. (2009) Holocene circum-Mediterranean vegetation changes: Climate forcing and human impact. *Quaternary International* 200: 4–18.

Jiménez-Espejo FJ, García-Alix A, Jiménez-Moreno G et al. (2014) Climate change and Saharan Aeolian input variations over Western Europe during the Holocene. *Chemical Geology* 374–375: 1–12.

Jiménez-Moreno G and Anderson RS (2012) Holocene vegetation and climate change recorded in alpine bog sediments from the Borreguiles de la Virgen, Sierra Nevada, southern Spain. *Quaternary Research* 77: 44–53.

Jiménez-Moreno G, Anderson RS, Atudorei V et al. (2011) A high-resolution record of vegetation, climate, and fire regimes in the mixed conifer forest of northern Colorado (USA). *Geological Society of America Bulletin* 123: 240–254.

Jiménez-Moreno G, García-Alix A, Hernández-Corbalán MD et al. (2013) Vegetation, fire, climate and human disturbance history in the southwestern Mediterranean area during the late Holocene. *Quaternary Research* 79: 110–122.

Kortekaas S and Dawson AG (2007) Distinguishing tsunami and storm deposits: An example from Martinhal, SW Portugal. *Sedimentary Geology* 200: 208–221.

Lario J, Zazo C, Goy JL et al. (2002) Changes in sedimentation trends in SW Iberia Holocene estuaries. *Quaternary International* 93–94: 171–176.

Laskar J, Robutel P, Joutel F et al. (2004) A long term numerical solution for the insolation quantities of the Earth. *Astronomy and Astrophysics* 428: 261–285.

Liu F and Feng Z (2012) A dramatic climatic transition at ≈4000 cal. yr BP and its cultural responses in Chinese cultural domains. *The Holocene* 22: 1–17.

López-Moreno JI, Vicente-Serrano SM, Moran-Tejeda E et al. (2011) Impact of climate evolution and land use changes on water yield in the Ebro basin. *Hydrology and Earth System Sciences* 15: 311–322.

Magny M (2004) Holocene climate variability as reflected by mid-European lake-level fluctuations and its probable impact on prehistoric human settlements. *Quaternary International* 113: 65–79.

Magny M, Joannin S, Galop D et al. (2012) Holocene palaeohydrological changes in the northern Mediterranean borderlands as reflected by the lake-level record of Lake Ledro, northeastern Italy. *Quaternary Research* 77: 382–396.

Marchal O, Cacho I, Stocker T et al. (2002) Apparent long-term cooling of the sea surface in the northeast Atlantic and Mediterranean during the Holocene. *Quaternary Science Reviews* 21: 455–483.

Martín-Puertas C, Jiménez-Espejo F, Martínez-Ruiz F et al. (2010) Late Holocene climate variability in the southwestern Mediterranean region: An integrated marine and terrestrial geochemical approach. *Climate of the Past* 6: 807–816.

Martín-Puertas C, Valero-Garcés BL, Mata MP et al. (2008) Arid and humid phases in southern Spain during the last 4000 years: The Zoñar Lake record, Cordoba. *The Holocene* 18: 907–921.

May W (2008) Potential future changes in the characteristics of daily precipitation in Europe simulated by the HIRHAM regional climate model. *Climate Dynamics* 30: 581–603.

Mayewski PA, Rohling EE, Stager JC et al. (2004) Holocene climate variability. *Quaternary Research* 62: 243–255.

Meijer PTh and Tuenter E (2007) The effect of precession-induced changes in the Mediterranean freshwater budget on circulation at shallow and intermediate depth. *Journal of Marine Systems* 68: 349–365.

Menéndez Amor J and Florschütz F (1964) Resultados del análisis paleobotánico de una capa de turba en las cercanías de Huelva (Andalucía). *Estudios Geológicos* 20: 183–186.

Moreno A, Pérez A, Frigola J et al. (2012) The Medieval Climate Anomaly in the Iberian Peninsula reconstructed from marine and lake records. *Quaternary Science Reviews* 42: 16–32.

Muñoz-Díaz D and Rodrigo FS (2003) Effects of the North Atlantic Oscillation on the probability for climatic categories of local monthly rainfall in southern Spain. *International Journal of Climatology* 23: 381–397.

Murray JW (2006) *Ecology and Applications of Benthic Foraminifera*. New York: Cambridge University Press, 426 pp.

Nissen KM, Leckebusch GC, Pinto JG et al. (2010) Cyclones causing wind storms in the Mediterranean: Characteristics, trends and links to large-scale patterns. *Natural Hazards and Earth System Sciences* 10: 1379–1391.

Paillard D, Labeyrie L and Yiou P (1996) Macintosh program performs time-series analysis. *Eos Trans. AGU* 77: 379.

Pérez-Asensio JN and Aguirre J (2010) Benthic foraminiferal assemblages in temperate coral-bearing deposits from the Late Pliocene. *Journal of Foraminiferal Research* 40: 61–78.

Pérez-Obiol R, Jalut G, Julià R et al. (2011) Mid-Holocene vegetation and climatic history of the Iberian Peninsula. *The Holocene* 21: 75–93.

Reed JM, Stevenson AC and Juggins S (2001) A multi-proxy record of Holocene climatic change in southwestern Spain: The Laguna de Medina, Cádiz. *The Holocene* 11: 707–719.

Reimer PJ, Baillie MGL, Bard E et al. (2009) IntCal09 and Marine09 radiocarbon age calibration curves, 0–50,000 years cal BP. *Radiocarbon* 51(4): 1111–1150.

Rivas-Martínez S (1987) *Memoria del mapa de series de vegetación de España*. Madrid: Ministerio de Agricultura, Pesca y Alimentación.

Rivas-Martínez S, Costa M, Castroviejo S et al. (1980) La vegetación de Doñana (Huelva, España). *Lazaroa* 2: 5–190.

Rodríguez-Ramírez A and Yáñez CM (2008) Formation of chenier plain of the Doñana marshland (SW Spain): Observations and geomorphic model. *Marine Geology* 254: 187–196.

Rodríguez-Ramírez A, Flores-Hurtado E, Contreras C et al. (2014) The role of neo-tectonics in the sedimentary infilling and geomorphological evolution of the Guadalquivir estuary (Gulf of Cadiz, SW Spain) during the Holocene. *Geomorphology* 219: 126–140.

Rodríguez-Ramírez A, Pérez-Asensio JN, Santos A et al. (in press) Atlantic extreme wave events in the Guadalquivir estuary (SW Spain) in the last four millennia BP: Regional implications. *Quaternary Research*.

Rodríguez-Ramírez A, Rodríguez-Vidal J, Cáceres L et al. (1996) Recent coastal evolution of the Doñana National Park (S. Spain). *Quaternary Science Reviews* 15: 803–809.

Rodríguez-Ramírez A, Ruiz F, Cáceres LM et al. (2003) Analysis of the recent storm record in the south-western Spain coast: Implications for littoral management. *Science of the Total Environment* 303: 189–201.

Ruiz F, González-Regalado ML, Pendón JG et al. (2005) Correlation between foraminifera and sedimentary environments in recent estuaries of southwestern Spain: Applications to Holocene reconstructions. *Quaternary International* 140–141: 21–36.

Ruiz Pessenda LC, Vidotto E, De Oliveira PE et al. (2012) Late Quaternary vegetation and coastal environmental changes at Ilha do Cardoso mangrove, southeastern Brazil. *Palaeogeography, Palaeoclimatology, Palaeoecology* 363–364: 57–68.

Salvany JM, Larrasoaña JC, Mediavilla C et al. (2011) Chronology and tectono-sedimentary evolution of the Upper Pliocene to Quaternary deposits of the lower Guadalquivir foreland basin, SW Spain. *Sedimentary Geology* 241: 22–39.

Santos L, Sánchez-Goñi MF, Freitas MC et al. (2003) Climatic and environmental changes in the Santo André coastal area (SW Portugal) during the last 15,000 years. In: Ruiz Zapata B, Dorado M, Valdeolmillos A et al. (eds) *Quaternary Climatic Changes and Environmental Crises in the Mediterranean Region*. Alcalá de Henares: Universidad de Alcalá, pp. 175–179.

Soares AMM and Martins JMM (2010) Radiocarbon dating of marine samples from Gulf of Cadiz: The reservoir effect. *Quaternary International* 221: 9–12.

Stevenson AC (1984) Studies on the vegetational history of S.W. Spain. III. Palynological investigations at El Asperillo, Huelva. *Journal of Biogeography* 11: 527–551.

Stevenson AC (1985) Studies in the vegetational history of SW Spain. II. Palynological investigations at Laguna de las Madres, Huelva. *Journal of Biogeography* 12: 293–314.

Stevenson AC and Harrison RJ (1992) Ancient forests in Spain. A model for land-use and dry forest management in S.W. Spain from 4000 BC to 1900 AD. *Proceedings of the Prehistoric Society* 58: 227–247.

Stevenson AC and Moore PD (1988) Studies in the vegetational history of S.W Spain. IV. Palynological investigation of valley mire at El Acebron, Huelva. *Journal of Biogeography* 15: 339–361.

Tuenter E, Weber SL, Hilgen FJ et al. (2003) The response of the African summer monsoon to remote and local forcing due to precession and obliquity. *Global and Planetary Change* 36: 219–235.

Tzedakis PC (2007) Seven ambiguities in the Mediterranean palaeoenvironmental narrative. *Quaternary Science Reviews* 26: 2042–2066.

Walker MJC, Berkelhammer M, Björck S et al. (2012) Formal subdivision of the Holocene series/epoch: A discussion paper by a working group of INTIMATE (Integration of ice-core, marine and terrestrial records) and the Subcommission on Quaternary Stratigraphy (International Commission on Stratigraphy). *Journal of Quaternary Science* 27: 649–659.

Wanner H, Solomina O, Grosjean M et al. (2011) Structure and origin of Holocene cold events. *Quaternary Science Reviews* 30: 3109–3123.

Weiss H, Courtney M-A, Wetterstrom W et al. (1993) The genesis and collapse of third millennium north Mesopotamian civilization. *Science* 261: 995–1004.

Yáñez C, Rodríguez A and Carrión JS (2006) Cambios en la vegetación de la franja littoral de las marismas de Doñana durante el Holoceno reciente. *Anales de Biología* 28: 85–94.

Yll EI, Zazo C, Goy JL et al. (2003) Quaternary palaeoenvironmental changes in South Spain. In: Ruiz-Zapata B, Dorado M, Valdeolmillos A et al. (eds) *Quaternary Climatic Changes and Environmental Crises in the Mediterranean Region*. Alcalá de Henares: Universidad de Alcalá, pp. 201–213.

Zazo C, Goy JL, Somoza L et al. (1994) Holocene sequence of sea-level fluctuations in relation to climatic trends in the Atlantic–Mediterranean linkage coast. *Journal of Coastal Research* 10: 933–945.

Zazo C, Mercier N, Silva PG et al. (2005) Landscape evolution and geodynamic controls in the Gulf of Cadiz (Huelva coast, SW Spain) during the Late Quaternary. *Geomorphology* 68: 269–290.